MEASUREMENTS AND MECHANISMS OF CRACK GROWTH AT ELEVATED TEMPERATURES UP TO 1273 K

K. Krompholz, E. D. Grosser, J. Böttner, and J. B. Pierick

INTERATOM
Internationale Atomreaktorbau GmbH
D-5060 Bergisch Gladbach 1, FRG

ABSTRACT

The potential drop method based on the compensation concept is used in measurements of crack growth behaviour of heat resistant alloys under static and cyclic loading in the high temperature range up to 1273 K. Test materials are cast alloys IN-519 and Manaurite 36 X and the wrought Ni-base materials Inconel 617, Nimonic 86, and Hastelloy X. The experiments are performed in air; the reproducibility of each measurement is proven by at least three CT-type samples.

The test results gained from cyclic loading experiments at a frequency of 5 Hz, R = 0.05, in air show the typical dependence of log(da/dN) upon log(ΔK). Reproducibility between samples was good and the onset to stable crack growth occured at a ΔK value of less than 10 MPa · $m^{1/2}$ at elevated temperatures.

The static load experiments are evaluated following the net stress concept; the applicability of linear elastic fracture mechanics seems doubtful for experiments lasting longer than 7.2 Ms (2,000 hours) at elevated temperatures. Nevertheless, the K-concept was applied to Inconel 617 for illustrative reasons.

KEYWORDS

Fatigue crack growth; creep crack growth; long term experiments; potential drop technique; elevated temperature application.

INTRODUCTION

The gasification of coal with nuclear energy needs materials which can withstand service temperatures of 1073 K to 1323 K. Although modern non-destructive techniques for flaw detection are capable of working at low detection limits, it must be assumed that components in practice will contain notches or flaws or develop cracks under service conditions. For components operating at elevated temperatures, it is possible that flaws present may grow by creep and/or fatigue.

In order to enable a reliable design it is urgently necessary to establish the factors controlling the crack propagation rate under fatigue and creep conditions. Experimental studies have shown that the processes of fatigue and creep crack growth consist of an initiation period and a growth period (Walton and Ellison, 1972; Weiss and Lal, 1974; Weiss, Rabaut, and MacInnes, 1969; Zaharia and Gershon, 1973; Crooker, 1976; Jack and Price, 1970; Lindley, Richards, and Ritchie, 1976; Plumbridge, 1972; Radon and Culver, 1976; Scarlin, 1975; Shahinian, 1978; Schijve, 1979; Neate and Siverns, 1974; Taira and Ohtani, 1974; Floreen, 1975; Haigh, 1975).

This presentation gives results of fatigue and creep crack growth investigations.

EXPERIMENTAL PROCEDURE

Fatigue Crack Growth Investigations

The fatigue crack growth investigations were performed on a closed loop servohydraulic computer-controlled MTS machine in air using load controlled with a sinusoidal waveform in tension. Before starting the experiments the samples were prefatigued. The length of the crack obtained by prefatigueing was measured by means of an optical microscope. Wires for current supply and for the potential drop measurement were connected to the specimen by electron beam welding using wires of the filler material: electrodes of Ni-base material. The specimens were heated by a three zone resistance-type furnace. For measuring the crack length the potential drop technique was used. The method and the test procedure were described elsewhere (Krompholz, Grosser, and Ewert, 1980). To avoid electrical short circuits via the load frame the load rods were electrically isolated outside the furnace. The evaluation of the tests was performed with a computer, type DEC PDP 11/04, using the 11-point incremental polynomial method, a method similar to that described by Clark and Hudak (1975).

The fatigue and creep crack growth specimen design is shown in Fig.1.

Creep Crack Growth Investigations

The experiments were performed under constant tensile load in air in creep machines of type TC 20 constructed by Mayes Ltd. As in the fatigue crack growth experiments, the specimens were heated by a three zone resistance furnace. The fatigue conditioning of the specimens and the method for the crack length measurement were the same as in the fatigue experiments. In these experiments the test data were analyzed graphically by calculating the time derivative of the plot of the crack length versus time for an instantaneous crack length a_i. Net stress was calculated from equation (5) and/or the stress intensity factor from equation (2), a method, which is described in detail by Clark and Hudak (1975) for fatigue crack growth investigations.

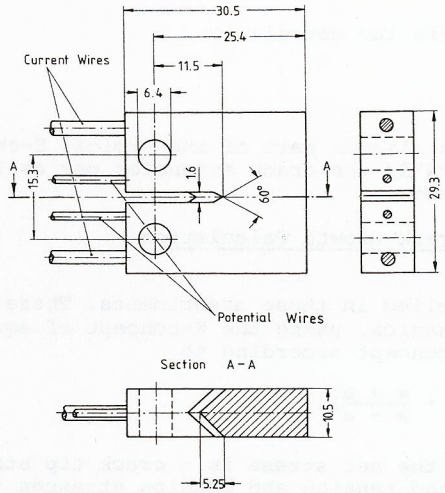

Fig. 1. CT-specimen with connections of the current and potential wires (all dimensions in mm)

DESCRIPTION OF EVALUATION PROCEDURES

Concept for Fatigue Crack Growth Calculation

The fatigue crack growth experiments were evaluated by means of the concept of linear elastic fracture mechanics using ΔK even at the highest temperature under investigation. The ΔK_I is calculated according to

$$\Delta K = K_{max} - K_{min} = K_{max} \cdot (1 - \frac{K_{min}}{K_{max}}) = K_{max} \cdot (1 - R), \qquad (1)$$

where R is the stress ratio. K_{max} can be calculated for the CT-specimen according to

$$K_{max} = \sigma_{n,max} \cdot a^{1/2} \cdot [29.6 - 185.5 \ (\frac{a}{w}) + 655.7 \ (\frac{a}{w})^2 - 1077.0 \ (\frac{a}{w})^3 + 638.9 \ (\frac{a}{w})^4] , \qquad (2)$$

where

$$\sigma_{n,max} = \frac{F_{max}}{B \cdot w} , \qquad (3)$$

is the nominal maximum stress, F_{max} the maximum load, B the thickness of the specimen, w the width of the specimen, and a the crack length.

The expression in brackets has been tabulated by Walker and May (1967).

In each case, the Paris law correlation

$$\frac{da}{dN} = C \cdot (\Delta K)^n , \qquad (4)$$

was calculated for the linear part of the typical S-shaped curve of the plots. Here, da/dN is the crack extension per cycle and C and n are calculated constants.

Concepts for Creep Crack Growth Calculation

Two concepts were applied in these experiments. These were (i) linear elastic fracture mechanics, using the K-concept of equation (2) and (ii) the net stress concept according to

$$\sigma_{net} = \frac{\sigma_n \cdot w}{w - a} \left(1 + 3 \cdot \frac{w + a}{w - a}\right). \qquad (5)$$

For the CT-specimen, the net stress is a crack tip stress calculated from the combined tension and bending stresses (Landes and Begley, 1976; Harrison and Sandor, 1971). The terms used are explained in equation (2) and (3).

Creep crack growth rates correlate also with the energy rate integral C^+, which is an adaption of the J-integral involving substitution of strain rates for strains and displacement rates for displacements. The method, which holds great promise for design calculations because C^+ can be calculated by finite element analysis as well as determined experimentally, is described in detail in literature (Landes and Begley, 1976; van Leeuwen, 1977; Riedel and Rice, 1979). Because of the technical equipment required, this last concept could not be applied in tests described here. In each case, results were analysed according to a power law

$$\frac{da}{dt} = A \cdot K^m, \qquad (6)$$

or the net stress model

$$\frac{da}{dt} = B \cdot (\sigma_{net})^b. \qquad (7)$$

Here, da/dt is the crack velocity and A, B, m, and b are constants.

RESULTS

The characterization of the test materials is given in Table 1. The test parameters are shown in Table 2. The evaluated fatigue data from Paris law, equation (4), are shown in Table 3.

Fatigue crack growth results for IN-519, Inconel 617, Nimonic 86, and Hastelloy X are shown in Figs. 2 - 5, respectively. The results are shown in the form of log(da/dN) vs. log(ΔK). Creep crack growth

TABLE 1 Characterization of Test Materials

Material	Heat	Chemical Composition (wt.%)												
		C	Si	Mn	Cr	Mo	Ni	V	W	Al	Co	Cu	Nb	Ti
IN - 519	345	.35	.73	.76	24.84	.03	24.97	.03	.06	<.004	.41	.01	1.62	<.01
Manaurite 36X	339	.43	.82	.89	25.44	.05	35.6	.04	.04	<.004	.37	.03	1.25	<.01
Manaurite 36X	346	.42	1.32	1.29	25.82	.22	33.4	.03	.02	<.004	.20	<.01	.84	<.01
Inconel 617	365	.065	.06	.0304	22.0	8.87	52.55	.09	.15	1.02	12.4	.21	.38	.33
Nimonic 86	376	.047	.19	.11	24.83	10.0	62.46	.09	.06	.039	.088	.04	<.01	.14
Hastelloy X	379	.079	.32	.69	21.34	8.74	45.4	.06	.69	.44	2.47	.02	.38	<.01

Material	Heat	Dimension (mm)	a_v / J (ISO - V)	ys / MPa	UTS / MPa
IN - 519	345	Φ134.8 × 17.7	7.2	232	456
Manaurite 36X	339	Φ134.2 × 17.35	8.0	255	496
Manaurite 36X	346	Φ134.8 × 17.7	8.6	274	531
Inconel 617	365	Φ 80 × 16.5	160	356	746
Nimonic 86	376	Φ 63.5	84.8	351	770
Hastelloy X	379	Φ 20.0	136	337	717

data for Inconel 617, evaluated as a function either of net stress or of stress intensity are given in Figs. 8 and 9, respectively, for 1123 K (850°C), 1173 K (900°C), 1223 K (950°C), and 1273 K (1000°C). Additionally, creep crack growth data from IN-519 and Manaurite 36 X as a function of the net stress applied is given in Fig. 7.

DISCUSSION

Discussion of the Fatigue Crack Growth Data

The fatigue crack growth behaviour of the alloys was investigated with the parameters as given in Table 2. At room temperature and in some cases at higher temperatures the load was lowered after reaching a crack velocity of $da/dN \approx 5 \cdot 10^{-4}$ mm/cycle, which leads to a slow

TABLE 2 Parameters for the Fatigue and Creep Crack Growth Investigations in Air for the Materials in the As-Received State

Material	Heat	Notch* Direction	R	f Hz	$\sigma_{n,max}$/MPa for T/K					
					308	1073	1123	1173	1223	1273
IN - 519	345	C - L	1	0	-	-	4.71 5.56	3.82	3.07	1.92 2.30 3.07
		C - L	0.05	5	12.8/8.6/6.4	8.6/6.4	8.6/6.4	6.4	5.1	4.3
Manaurite 36 X	339	C - L	1	0	-	-	4.14, 4.15	4.51	-	-
	346	C - L	1	0	-	-	4.52	3.76; 4.54	-	-
Inconel 617	365	C - L	1	0	-	-	6.41	4.94 4.90	4.09 2.97 2.95 4.12	2.24;1.86
		C - L	0.05	5	11.5/9.6/5.8	5.0	5.0	4.6	3.8	3.8
Nimonic 86	376	C - R	0.05	5	13.1/ 9.4	4.9	4.1	3.8	3.4	3.4
Hastelloy X	379	T - L	0.05	5	11.4/ 7.6	5.3	3.8	3.8	3.4	3.2

*According to ASTM - E399 - 74

Figures given in the Table refer to nominal stress (MPa) applied

shift of the total curve towards higher crack velocities. This was observed at room temperature, where a constant R-value and three different loads were used in one experiment to obtain the full curve da/dN vs. ΔK.

Figs. 2 - 5 show the experimental results obtained at 308 K (35°C), 1073 K (800°C), 1123 K (850°C), 1173 K (900°C), 1223 K (950°C), and 1273 K (1000°C) for the alloys IN-519, Inconel 617, Nimonic 86, and Hastelloy X. The curves shown were derived from the best fit of the evaluated points.

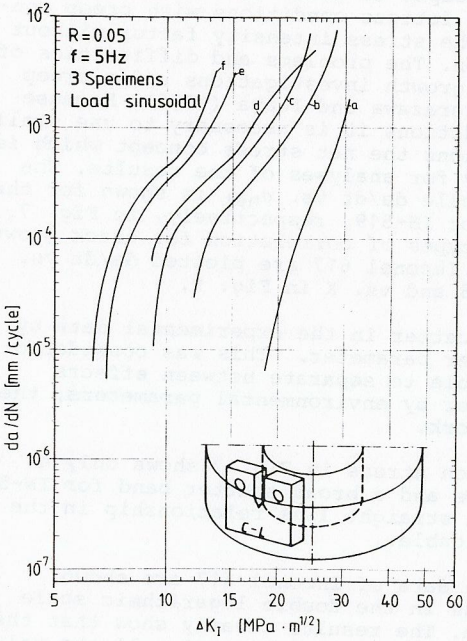

Fig. 2. Fatigue crack growth rates vs. stress intensity for G-X 35 CrNi 24 24 (IN-519); f = 5 Hz, load controlled with sinusoidal load in tension, R = 0.05; a: 308 K, b: 1073 K, c: 1123 K, d: 1173 K, e: 1223 K, f: 1273 K

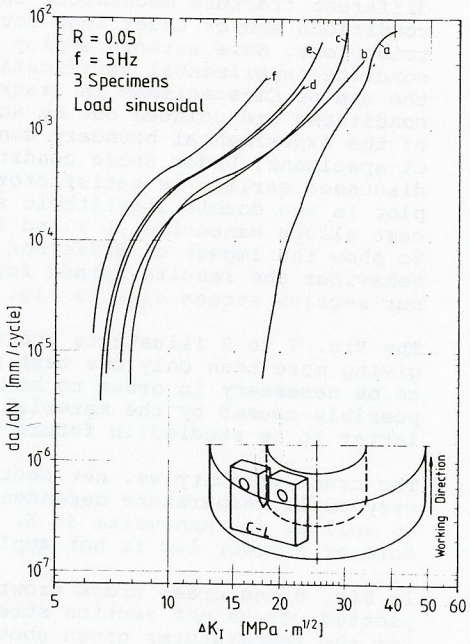

Fig. 3. Fatigue crack growth rates vs. stress intensity for Inconel 617, f = 5 Hz, load controlled with sinusoidal load in tension, R = 0.05; a: 308 K, b: 1073 K, c: 1123 K, d: 1173 K, e: 1223 K, f: 1273 K

Fig. 6 shows the typical narrow scatter of the data measured at e.g. 1273 K (1000°C) for Inconel 617. The reproducibility was always checked with three specimens. Between room temperature (308 K) and 1273 K exists a very distinct temperature shift in the curves da/dN vs. ΔK. In nearly all experiments a determination of ΔK_C, a value, at which the crack starts to propagate unstable, was directly possible from the typical S-shaped curves.

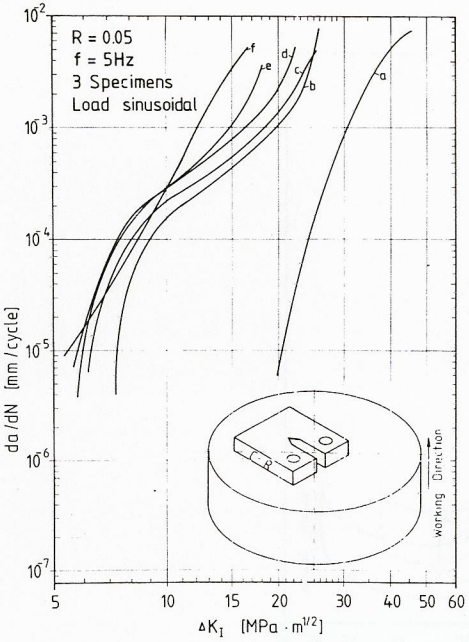

Fig. 4. Fatigue crack growth rates vs. stress intensity for Nimonic 86, f = 5 Hz, load controlled with sinusoidal load in tension, R = 0.05; a: 308 K, b: 1073 K, c: 1123 K, d: 1173 K, e: 1223 K, f: 1273 K

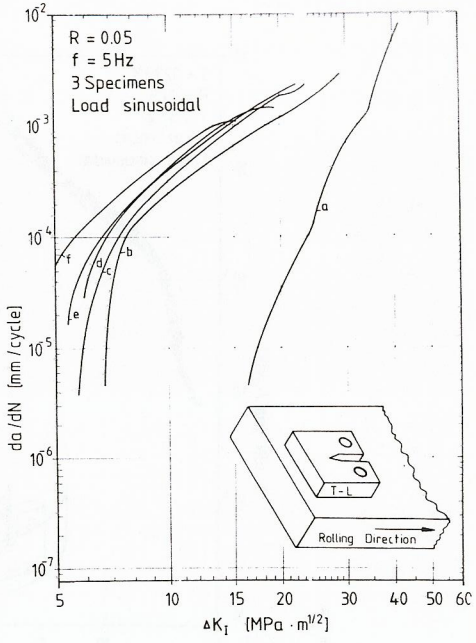

Fig. 5: Fatigue crack growth rates vs. stress intensity for S-NiCr 21 Fe 18 Mo (Hastelloy X); f = 5 Hz, load controlled with sinusoidal load in tension, R = 0.05; a: 308 K, b: 1073 K, c: 1123 K, d: 1173 K, e: 1223 K, f: 1273 K

In all cases the specimen size according to ASTM Designation E 647-78 T was violated with respect to the uncracked ligament. That is because larger specimens are not suitable in planned investigations under different environments for fatigue and creep crack growth studies. So in some special cases the load point deflection was measured additionally to show that the recommended procedure for specimens violating section 7.2 was fulfilled. Tests have shown that even at 1223 K and 1273 K the application of linear elastic fracture mechanics is possible for small specimens of these materials; results of these investigations will be published elsewhere.

The fatigue crack growth rates vs. stress intensity amplitudes were fitted by least square regression analysis of the experimental data according to equation (4). The parameters C and n are given in Table 3.

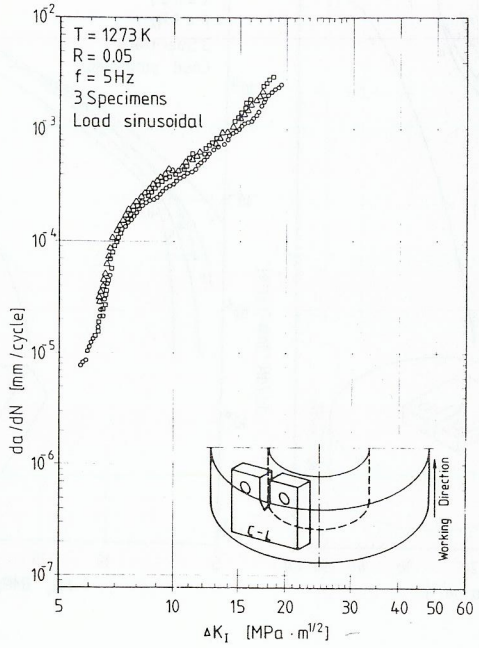

Fig. 6. Fatigue crack growth rates vs. stress intensity for Inconel 617; f = 5 Hz, load controlled with sinusoidal load in tension, R = 0.05; example for T = 1273 K

TABLE 3 Parameters C and n, Calculated by Least Square Analysis from Equation (4)

Material	Heat	C, n acc. to equ. (4)	T/K 308	1073	1123	1173	1223	1273
IN - 519	345	C	$2 \cdot 10^{-16}$	$8.22 \cdot 10^{-10}$	$2.94 \cdot 10^{-8}$	$3.44 \cdot 10^{-8}$	$1.52 \cdot 10^{-8}$	$2.56 \cdot 10^{-8}$
		n	8.41	4.60	3.54	3.55	4.28	4.26
Inconel 617	365	C	$2.88 \cdot 10^{-17}$	$1.32 \cdot 10^{-6}$	$1.47 \cdot 10^{-6}$	$2.86 \cdot 10^{-6}$	$1.19 \cdot 10^{-6}$	$1.05 \cdot 10^{-6}$
		n	8.91	2.06	2.05	1.94	2.31	2.57
Nimonic 86	376	C	$1.14 \cdot 10^{-17}$	$4.20 \cdot 10^{-7}$	$8.37 \cdot 10^{-7}$	$9.93 \cdot 10^{-7}$	$7.26 \cdot 10^{-7}$	$3.52 \cdot 10^{-9}$
		n	9.20	2.53	2.41	2.42	2.59	4.77
Hastelloy X	379	C	$4.03 \cdot 10^{-15}$	$1.37 \cdot 10^{-6}$	$7.83 \cdot 10^{-7}$	$7.22 \cdot 10^{-7}$	$7.79 \cdot 10^{-7}$	$1.12 \cdot 10^{-6}$
		n	7.40	2.23	2.60	2.69	2.67	2.61

It should be mentioned, that at such high temperatures the interaction of creep and fatigue becomes important. For this reason a high frequency of about 5 Hz was chosen to give short term tests (up to 36 ks (10 h)) and reduce the effect of the interaction to give some scope for the application of linear elastic fracture mechanics.

Discussion of the Creep Crack Growth Data

While conducting these experiments the authors noticed that very little experimental evidence is available on the applicability of different fracture mechanical concepts to crack growth under creep conditions and/or under long term fatigue conditions with creep contributions. Some authors employ the stress intensity factor without concrete experimental verification. The problems and difficulties of the use of CT-specimens in crack growth investigations under creep conditions are pointed out by Koterazawa and Iwata (1976). Because of the experimental boundary conditions it is necessary to use small CT-specimens. Under those conditions the net stress concept which is discussed earlier is satisfactory for analyses of the results. The plot in the double logarithmic scale da/dt vs. σ_{net} is shown for the cast alloys Manaurite 36 X and for IN-519, respectively, in Fig. 7. To show the impact of different types of correlation for crack growth behaviour the results gained for Inconel 617 are plotted da/dt vs. net section stress σ_{net} in Fig. 8 and vs. K in Fig. 9.

The Fig. 7 to 9 illustrate the scatter in the experimental data by giving more than only one test per parameter. This was considered to be necessary in order to be able to separate between effects possibly caused by the material or by environmental parameters, the latter to be studied in future work.

The crack velocity vs. net section stress in Fig. 7 shows only a very small temperature dependence and a broad scatter band for IN-519 as well as for Manaurite 36 X. A straight line relationship in the form of a power law is not applicable.

In Fig. 8 the creep crack growth data of Inconel 617 are shown plotted versus net section stress in the double logarithmic scale for the temperatures given above. The results clearly show that the scatter of the values obtained at 1273 K covers nearly all the values from the experiments at lower temperatures. In the net section stress concept there is no clear temperature dependence. However, the curves for 1123 K cross those for 1173 K and 1223 K at σ_{net} = 300 MPa, so that at higher stresses crack growth is faster at lower temperatures. This might be due to differences in net section yielding. An alternative explanation for the cross-over behaviour is that, at the higher temperatures, crack growth may be effected by dynamic oxidation within the growing crack.

To compare these results with linear elastic fracture mechanical concept da/dt is plotted versus K_I in Fig. 9 at the same temperatures as discussed in Fig. 8. Using the net section stress from Fig. 8 and comparing it with the linear elastic fracture mechanical concept used in Fig. 9, it can be shown that there is a clear temperature dependence for results at 1123 K, 1173 K, and 1223 K. Only the results obtained at 1273 K deviate from this temperature dependence; the crack velocities are about an order of magnitude lower than expected from the data at lower temperature. This effect

could be explained by oxidation within the growing cracks which might also account for the early cross over effects, as mentioned above.

The picture of the fracture surface is totally different from that of the fatigue crack in all cases. In creep crack growth yielding plays an important role. Crack propagation is accompanied by ligament necking according to yielding so that K seems inadequate to describe creep crack growth. Fig. 8 as well as Fig. 9 clearly show that there is no straight line relationship between crack growth rate and net section stress or K, respectively.

For this reason is seems urgently necessary to find an improved model. This model should be applicable for fatigue as well as for creep crack growth investigations so to reflect the mutual interaction between these two processes.

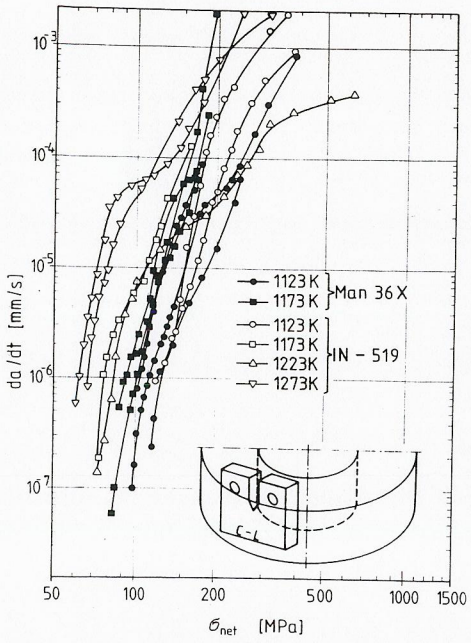

Fig. 7. Creep crack growth rates vs. net section stress for the cast alloys Manaurite 36 X and IN-519 for different temperatures

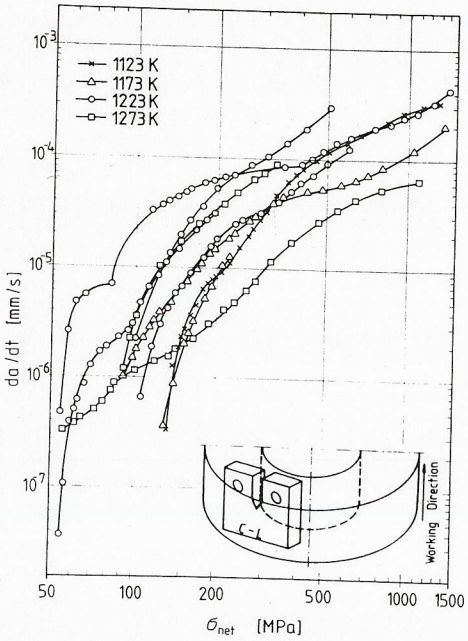

Fig. 8. Creep crack growth rates vs. net section stress for the wrought alloy Inconel 617 for different temperatures

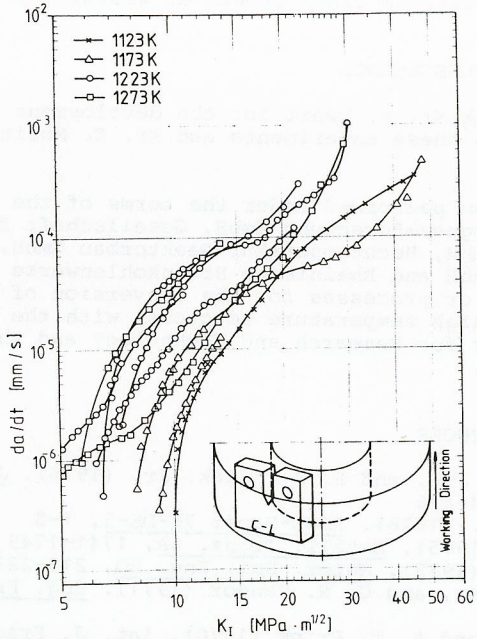

Fig. 9. Creep crack growth rates vs. stress intensity K_I for the wrought alloy Inconel 617 for different temperatures

CONCLUSION

The experimental results for fatigue crack growth from short term experiments show a high reproducibility as well as a plane fracture surface. One can conclude the concept of linear elastic fracture mechanics even at the highest temperature under investigation (i.e. 1273 K) seems to be applicable.

There is a limited possibility to compare the data with literature information. At 1123 K results for the Ni-base alloy IN-738 from fatigue crack growth experiments have been reported elsewhere. The results are close to those for IN-519 with respect to fatigue crack growth but the temperature dependence is more pronounced for these alloys than for IN-738 investigated at 1023 K and 1123 K.

The results of the fatigue crack growth experiments clearly show that the potential drop technique has proven to be a useful tool for measuring crack growth even at very high temperatures.

In creep crack growth investigations the results show a large scatter. The concepts used for the description of phenomena; i.e. σ_{net} as well as K, seem not to be reasonable for long term experiments, i.e. for

experiments lasting longer than 7.2 Ms (2,000 hours). The results clearly show that there is a need for an improved concept which combines creep and fatigue crack growth at elevated temperatures.

ACKNOWLEDGEMENTS

The authors thank Mr. K. Ewert for the development of the computer programs used in these experiments and Mr. E. Moritz for experimental support.

The work has been performed under the terms of the cooperative agreement between Bergbau-Forschung GmbH, Gesellschaft für Hochtemperatur-reaktortechnik mbH, Hochtemperatur-Reaktorbau GmbH, Kernforschungsanlage Jülich GmbH and Rheinische Braunkohlenwerke AG dealing with the development or processes for the conversion of solid fossil fuels with heat from high temperature reactors, with the assistance of the Federal Minister for Research and Technology and the State of Nordrhein-Westfalen.

REFERENCES

- Clark, W. G., Jr., and S. J. Hudak, Jr. (1975). Journal Test. Eval. 3, 454-476
- Crooker, T. W. (1976). ASME-Paper 76-DE-5, 1-8
- Floreen, S. (1975). Metall. Trans. 6A, 1741-1749
- Haigh, J. R. (1975). Mater. Sci. Eng. 20, 213-223
- Harrison, C. B., and G. N. Sandor (1971). Eng. Fracture Mech. 3, 403-420
- Jack, A. R., and A. T. Price (1970). Int. J. Fracture Mech. 6, 401-409
- Koterazawa, R., and Y. Iwata (1976). Trans. ASME J. Eng. Mater. Techn. 296-304
- Krompholz, K., E. D. Grosser, and K. Ewert (1980). Z. Werkstofftechn. 11, 60-67
- Landes, J. D., and J. A. Begley (1976). ASTM STP 590, 128-148
- Lindley, T. C., C. E. Richards, and R. O. Ritchie (1976). Metallurgia Metal Form. 43, 268-280
- Neate, G. J., and M. J. Siverns (1974). Creep and Fatigue in Elevated Temp. Appl. Intern. Conference Philadelphia, Sept. 1973, Sheffield 1974 C 234/73
- Plumbridge, W. J. (1972). J. Mater. Sci. 7, 939-962
- Radon, J. C., and L. E. Culver (1976). Experimental Mech., 105-110
- Riedel, H., and J. R. Rice, Tensile Cracks in Creeping Solids, presented at the ASTM Annual Symp. on Fracture Mechanics, St. Louis, May 1979
- Scarlin, R. B. (1975). Mater. Sci. Eng. 21, 139-147
- Schijve, J. (1979). Eng. Fracture Mech. 11, 167-221
- Shahinian, P. (1978). Metals Techn. 372-380
- Taira, S., and R. Ohtani (1974). Creep and Fatigue in Elevated Temp. Appl. Intern. Conference Philadelphia Sept. 1973, Sheffield 1974 C 213/73
- van Leeuwen, H. P. (1977). Eng. Fracture Mech. 9, 951-974
- Walker, E. F., and M. J. May (1967). BISRA Open Report PB 180453 MG/E/307/67

- Walton, D., and E. G. Ellison (1972). Intern. Metall. Reviews, 17, 100-116
- Weiss, V., and D. N. Lal (1974). Metall. Trans. 5, 1946-1949
- Weiss, V., G. Rabaut, and W. MacInnes (1969). Czech. J. Phys. B 18, 351-361
- Zaharia, C., and P. Gershon (1973). Isr. J. Technol. 11, 287-290